Discussion Paper No.286

Neoclassical Growth Model with Multiple Distributed Delays

Luca Guerrini
Polytechnic University of Marche

Akio Matsumoto
Chuo University

Ferenc Szidarovszky
University of Pécs

October 2017

INSTITUTE OF ECONOMIC RESEARCH
Chuo University
Tokyo, Japan

Neoclassical Growth Model with Multiple Distributed Delays*

Luca Guerrini[†] Akio Matsumoto[‡] Ferenc Szidarovszky[§]

Abstract

This paper demonstrates that the delay has a dual effects of being destabilizer and stabilizer. For this purpose, we use a traditional neoclassical growth model augmented with two continuously distributed time delays, time-to-build delay and time-to-depreciate delay. Applying the Routh-Hurwitz stability criterion, we first construct a condition under which a stationary state loses stability and bifurcates to a cyclic oscillations. It is then numerically demonstrated that the delay has the dual effects: the main role of the delay is to destabilize an otherwise stable economy and it is found that the delay can also stabilize the economy, depending on the combination of two delays. The dual effect is specific to a two delay dynamic model.

Keywords: Continuously distributed time delay, Neoclassical growth model, Dual effect, Two delays

*The second author highly acknowledges the financial supports from the MEXT-Supported Program for the Strategic Research Foundation at Private Universities 2013-2017, the Japan Society for the Promotion of Science (Grant-in-Aid for Scientific Research (C) 25380238, 26380316 and 16K03556) and Chuo University (Joint Research Grant). The usual disclaimers apply.

[†]Department of Management, Polytechnic University of Marche, 60121 Ancona, Italy. luca.guerrini@staff,univpm.it

[‡]Department of Economics, Chuo University, 742-1, Higashi-Nakano, Hachioji, Tokyo 192-0393, Japan. akiom@tamacc.chuo-u.ac.jp

[§]Department of Applied Mathematics, University of Pécs, Ifjúság u 6, 7624 Pécs, Hungary. szidarka@gmail.com

1 Introduction

The seminal work of Kalecki (1935) indicates that a delay inevitably occurred in economic activities can be an essential source of macroeconomic dynamics. After a long "gestation period" in which only a limited works on delay dynamics have been done, it has been demonstrated in the recent literature that capital accumulation in a continuous-time framework could be cyclic or chaotic. This finding indicates that a delay equilibrium model of a dynamic economy may explain a wide variety of dynamics behavior ranging from simple convergence to erratic oscillations. In particular, Zak (1999) rebuilds the neoclassical growth model of Solow and Swan in such a way that the current capital stock is adjusted by the savings and the stock depreciation at some preceding time and shows two main results: one is that stable equilibrium of the traditional neoclassical growth model becomes a saddle point and the other is that endogenous cycle can emerge if the initial point can be taken from a center manifold. Matsumoto and Szidarovsky (2011, 2013) reconsider the discrete-time model of Day (1982) in the continuous time framework augmented with a production delay and numerically confirm the birth of complex dynamics involving chaos through ala period-doubling cascade. Bianca et al. (2013) generalize Zak's version of the neoclassical model by introducing two delays. Only recently Guerrini et al. (2017) apply the method developed by Gu et al. (2005) for the two delay model and construct a conditions under which a steady state loses stability or gains stability.

There are two types of delay, fixed time delay and continuously distributed time delay (fixed delay and continuous delay henceforth). The former is applicable in economic situations in which an institutionally or socially determined fixed period of time delay is presented. The latter is appropriate for economic situations in which different lengths of delays are distributed over the different economic agents. The choice of the type has situation-dependency. The neoclassical growth model is usually considered to describe *Robinson Crusoe* economy in which Robinson has two faces, he is a household and at the same time, a producer. In such a one-man economy fixed delay is most appropriate. We should remember that the neoclassical model itself has dual nature. It can be considered to possess a general equilibrium structure in which many households and many producers are involved and make trade of their outputs through markets. In the existing literature, however, applications of continuous delays are so far very few. It has not yet been determined whether or not cyclic capital accumulation may appear in the case in which fixed delays are replaced with continuous delays. The main propose of this study is to demonstrate the possibility of cyclic or possibly erratic capital accumulation under continuous delays.

The rest of the paper is organized as follows. Section 2 constructs a continuous delay version of the neoclassical growth model and discusses dynamics of two special cases, one with no delays and the other has two delays whose weighting function is exponentially declining. Section 3 examines the case in which the delay associated with production has weak delay kernel and the delay associated with capital depreciation has strong delay kernel. In Section 4 the weak and strong kernels are interchanged. Finally Section 5 provides concluding remarks.

2 The model

Zak (1999) introduced a discrete time delay into the Solow model and obtained the following delay differential equation

$$\dot{k}(t) = sk^{\alpha}(t-\tau) - \delta k(t-\tau), \tag{1}$$

where k denotes capital stock, α is a constant with $0 < \alpha < 1$, $s \in (0, 1)$ is a constant saving rate, $\delta > 0$ is capital depreciation, and $\tau > 0$ represents a time delay. It is well known that dynamical systems with distributed delay are more general than those with discrete delay. So we propose the following Solow model with distributed delays

$$\dot{k}(t) = s\left[\int_{-\infty}^{t} W(t-r, S, m)k(r)dr\right]^{\alpha} - \delta \int_{-\infty}^{t} W(t-r, T, n)k(r)dr, \tag{2}$$

where m and n are nonnegative integers, T and S are positive real parameters, and the delay kernel W is given by the gamma-type distribution

$$W(t-r, \zeta, l) = \left(\frac{l+1}{\zeta}\right)^{l+1} \frac{(t-r)^l e^{-\frac{(l+1)}{\zeta}(t-r)}}{l!}.$$

for $\zeta = S, T$ and $l = m, n$. Parameter ζ is associated with the average length of the continuous delay and l determines the shape of the weighting function. The two special cases $l = 0$ and $l = 1$ are called *weak delay kernel* and *strong delay kernel*, respectively. Notice that as $\zeta \to 0$ the distribution function approaches the Dirac distribution. Thus, one recovers the discrete delay case.

Letting $x(t) = k(t) - k_*$ transfers $k = k_*$ to the origin, where k_* is the non-trivial equilibrium of (1), namely k_* is the unique solution of $sk_*^{\alpha-1} = \delta$. The linearized equation of (2) at the origin has the form

$$\dot{x}(t) = \alpha\delta \int_{-\infty}^{t} W(t-r, S, m)x(r)dr - \delta \int_{-\infty}^{t} W(t-r, T, n)x(r)dr. \tag{3}$$

In Eq. (3), we look for the solution in the exponential form $x(t) = x(0)e^{\lambda t}$ to obtain the associated characteristic equation, which is given by

$$\lambda - \alpha\delta \int_{-\infty}^{t} W(t-r, S, m)e^{-\lambda(t-r)}dr + \delta \int_{-\infty}^{t} W(t-r, T, n)e^{-\lambda(t-r)}dr = 0. \tag{4}$$

Introducing the new variable $z = t - r$, and using the definition of the Gamma function, we get

$$\begin{aligned} \int_{-\infty}^{t} W(t-r, \zeta, l)e^{-\lambda(t-r)}dr &= \int_{0}^{+\infty} W(z, \zeta, l)e^{-\lambda z}dz \\ &= \left(\frac{l+1}{\zeta}\right)^{l+1} \frac{1}{l!} \int_{0}^{+\infty} z^l e^{-\left(\frac{l+1}{\zeta}+\lambda\right)z}dz \\ &= \left(1 + \frac{\lambda\zeta}{l+1}\right)^{-(l+1)}. \end{aligned}$$

Using this relation in (4), the characteristic equation becomes

$$\lambda - \alpha\delta\left(1 + \frac{\lambda S}{m+1}\right)^{-(m+1)} + \delta\left(1 + \frac{\lambda T}{n+1}\right)^{-(n+1)} = 0. \tag{5}$$

Eq. (5) is a polynomial equation with degree $m+n+3$ that can be represented as follows:

$$b_0\lambda^N + b_1\lambda^{N-1} + \cdots + b_{N-1}\lambda + b_N = 0, \tag{6}$$

where the coefficients b_j are real constants and $N = m+n+3$. We can easily guarantee that $b_0 > 0$. The Routh-Hurwitz theorem provides conditions that are both necessary and sufficient for this polynomial to have roots with negative real parts. In order to apply this theorem, we first need to construct the $N \times N$ Routh-Hurwitz matrix

$$\Delta_N = \begin{bmatrix} b_1 & b_0 & 0 & 0 & \cdots & 0 \\ b_3 & b_2 & b_1 & b_0 & \cdots & 0 \\ b_5 & b_4 & b_3 & b_2 & \cdots & 0 \\ \vdots & \vdots & \vdots & \vdots & \cdots & \vdots \\ 0 & 0 & 0 & 0 & \cdots & b_N \end{bmatrix}, \tag{7}$$

where $b_k = 0$ for $k > N$. The Routh-Hurwitz criterion states that all of the roots of Eq. (6) are negative or have negative real part if and only if all the principal minors Δ_N^k $(k = 1, 2, ..., N)$ of the Routh-Hurwitz matrix (7) are positive. A direct consequence of the Routh-Hurwitz theorem is that all coefficients b_k $(k = 1, 2, ..., N)$ are positive.

Since it is difficult to obtain a general solution of Eq. (5) we draw attention to some special cases and examine stability of the equilibrium analytically as well as numerically. Before proceeding, we examine two cases, one for $S = T = 0$ and the other for $m = n = 0$. In the former case, we immediately obtain the solution $\lambda = -(1-\alpha)\delta < 0$, and thus the equilibrium is locally asymptotically stable in absence of delays. In the latter case in which both delays have exponentially declining weights, the characteristic equation (5) becomes a cubic equation in λ,

$$b_0\lambda^3 + b_1\lambda^2 + b_2\lambda + b_3 = 0 \tag{8}$$

with

$$\begin{aligned} b_0 &= b_0(S,T) = ST > 0, \\ b_1 &= b_1(S,T) = S + T > 0, \\ b_2 &= b_2(S,T) = 1 + \delta S - \alpha\delta T, \\ b_3 &= b_3(S,T) = (1-\alpha)\delta > 0. \end{aligned}$$

According to the Routh-Hurwitz criterion, since $b_1b_2 > b_0b_3,\ b_0 > 0,\ b_1 > 0$ and $b_3 > 0$ implies $b_2 > 0$, the stability condition is validated if $b_1b_2 > b_0b_3$. A direct calculation shows this to hold when

$$\alpha\delta T^2 - T - S(1+\delta S) < 0$$

or

$$0 < T < \frac{1 + \sqrt{1 + 4\alpha\delta S(1+\delta S)}}{2\alpha\delta} = T_*.$$

Notice that the other solution is negative as $1 - \sqrt{1 + 4\alpha\delta S(1+\delta S)} < 0$. According to the Hopf bifurcation theorem, one can establish the existence of a cyclic solution at $T = T_*$ if the characteristic equation (8) has a pair of purely imaginary roots and the real parts of these roots change signs with T which is selected as the bifurcation parameter. When $T = T_*$, one has

$$b_1^* b_2^* = b_0^* b_3^*,$$

where $b_j^* = b_j(S, T_*)$ $(j = 0, 1, 2, 3)$, and so Eq. (8) factors as

$$\left(b_0^*\lambda + b_1^*\right)\left(b_0^*\lambda^2 + b_2^*\right) = 0,$$

yielding a pair of purely imaginary roots

$$\lambda_{1,2} = \pm i\omega_* \text{ with } \omega_* = \sqrt{\frac{b_2^*}{b_0^*}} > 0$$

and a real root

$$\lambda_3 = -\frac{b_1^*}{b_0^*} < 0.$$

Differentiating Eq. (8) with respect to T, we have

$$\frac{d\lambda}{dT} = -\frac{b_0'\lambda^3 + b_1'\lambda^2 + b_2'\lambda}{3b_0\lambda^2 + 2b_1\lambda + b_2}, \tag{9}$$

with

$$b_0' = b_0'(S,T) = S, \quad b_1' = b_1'(S,T) = 1, \quad b_2' = b_2'(S,T) = -\alpha\delta.$$

It is clear that $\lambda = i\omega_*$ is a simple root of (8), since (8) is cubic and we forward all of its three roots, which are different. Using (8) one has that (9) becomes

$$\frac{d\lambda}{dT} = \frac{\left(b_0'b_1 - b_0b_1'\right)\lambda^2 + \left(b_0'b_2 - b_0b_2'\right)\lambda + b_0'b_3}{3b_0^2\lambda^2 + 2b_0b_1\lambda + b_0b_2}.$$

Recalling $\omega_*^2 = b_2^*/b_0^*$ and $b_1^*b_2^* = b_0^*b_3^*$, we derive

$$\text{Re}\left(\frac{d\lambda}{dT}\right)_{\lambda=i\omega_*} = \frac{b_0'^*b_1^*b_2^* - b_0^*b_1'^*b_2^* - b_0^*b_1^*b_2'^*}{2b_0^*(b_0^*b_2^* + b_1^{*2})}.$$

Since the numerator of the above expression is equal to $S[\alpha\delta T_*^2 + S(1 + \delta S)] > 0$, only crossing the imaginary axis from left to right is possible as T increases. Thus, stability of the equilibrium is lost and the system remains unstable for all $T > T_*$. The previous analysis can be summarized as follows.

Theorem 1 *Given $m = n = 0$, the equilibrium point k_* of (2) is locally asymptotically stable for $T < T_*$, unstable for $T > T_*$ and bifurcates to a limit cycle through a Hopf bifurcation at k_* when $T = T_*$.*

3 Heterogenous weights I: $m = 0$ and $n \geq 1$

We now consider the case of $m = 0$ and $n \geq 1$ under which delay T has a bell-shaped weight while delay S has a declining weight. Substituting $m = 0$ reduces the characteristic equation (5) to

$$\lambda - \alpha\delta\left(1 + \lambda S\right)^{-1} + \delta\left(1 + \frac{\lambda T}{n+1}\right)^{-(n+1)} = 0.$$

or

$$[\lambda(1+\lambda S)-\alpha\delta]\left(1+\frac{\lambda T}{n+1}\right)^{n+1}+\delta(1+\lambda S)=0.$$

With expanding the factored terms, this can be rewritten as a polynomial equation of degree $n+3$,

$$b_0\lambda^{n+3}+b_1\lambda^{n+2}+\cdots+b_{n+2}\lambda+b_{n+3}=0 \tag{10}$$

where the coefficients are defined by

$$\begin{aligned}
b_0 &= a_0 S,\\
b_1 &= a_1 S + a_0,\\
b_k &= a_k S + a_{k-1} - \alpha\delta a_{k-2} \text{ for } 2 \le k \le n+1,\\
b_{n+2} &= 1+\delta S-\alpha\delta T,\\
b_{n+3} &= (1-\alpha)\delta > 0
\end{aligned}$$

with

$$a_k=\left(\frac{T}{n+1}\right)^{n+1-k}\binom{n+1}{k}. \tag{11}$$

3.1 $m=0$ and $n=1$

For $m=0$ and $n=1$, the characteristic equation (10) takes the form

$$b_0\lambda^4+b_1\lambda^3+b_2\lambda^2+b_3\lambda+b_4=0 \tag{12}$$

where

$$\begin{aligned}
b_0 &= b_0(S,T)=\frac{T^2}{4}S>0,\\
b_1 &= b_1(S,T)=TS+\frac{T^2}{4}>0,\\
b_2 &= b_2(S,T)=S+T-\alpha\delta\frac{T^2}{4},\\
b_3 &= b_3(S,T)=1+\delta S-\alpha\delta T,\\
b_4 &= b_4(S,T)=(1-\alpha)\delta>0.
\end{aligned}$$

The Routh-Hurwitz criterion now yields the conditions $b_3>0$, i.e. $\alpha<(1+\delta S)/(\delta T)$, and

$$\Delta_4^3(T)=b_1b_2b_3-b_0b_3^2-b_1^2b_4>0,$$

since they imply $b_2>0$ as well.

Let $\lambda_1,\lambda_2,\lambda_3$ and λ_4 denote the roots of Eq. (12). Then, we have

$$\lambda_1+\lambda_2+\lambda_3+\lambda_4=-\frac{b_1}{b_0},\quad \lambda_1\lambda_2+\lambda_1\lambda_3+\lambda_1\lambda_4+\lambda_2\lambda_3+\lambda_2\lambda_4+\lambda_3\lambda_4=\frac{b_2}{b_0}, \tag{13}$$

$$\lambda_1\lambda_2\lambda_3+\lambda_1\lambda_3\lambda_4+\lambda_2\lambda_3\lambda_4+\lambda_1\lambda_2\lambda_4=-\frac{b_3}{b_0},\quad \lambda_1\lambda_2\lambda_3\lambda_4=\frac{b_4}{b_0}. \tag{14}$$

If there is $T = T_*$ such that $\Delta_4^3(T_*) = 0$, by the Routh–Hurwitz criterion at least one root of Eq. (12), say λ_1, has real part equal to zero. As a result, the fourth equation of (14) implies $\operatorname{Im}\lambda_1 = \omega_1 \neq 0$. Thus, there exists another root of Eq.(12), say λ_2, such that $\lambda_2 = \bar{\lambda}_1$. Since $\Delta_4^3(T)$ is a continuous function of its roots, we conclude that λ_1 and λ_2 are complex conjugates in an open interval including T_*. Consequently, Eqs. (13) and (14) at $T = T_*$ rewrite as

$$\lambda_3 + \lambda_4 = -\frac{b_1}{b_0}, \quad \omega_1^2 + \lambda_3\lambda_4 = \frac{b_2}{b_0}, \quad \omega_1^2 (\lambda_3 + \lambda_4) = -\frac{b_3}{b_0}, \quad \omega_1^2\lambda_3\lambda_4 = \frac{b_4}{b_0}. \tag{15}$$

If the roots λ_3 and λ_4 are complex conjugates, then the first equation of (15) yields $2\operatorname{Re}\lambda_3 = -b_1/b_0 < 0$. On the other hand, if the roots λ_3 and λ_4 are real, then the first and fourth equations of (15) lead us to $\lambda_3 < 0$ and $\lambda_4 < 0$.

We need to check the transversality condition. For computational purposes, we multiply both sides of Eq. (12) by b_0^{-1} and obtain

$$\lambda^4 + \frac{b_1}{b_0}\lambda^3 + \frac{b_2}{b_0}\lambda^2 + \frac{b_3}{b_0}\lambda + \frac{b_4}{b_0} = 0.$$

Differentiating this equation with respect to T, one has

$$\frac{d\lambda}{dT} = -\frac{\left(\frac{b_1}{b_0}\right)'\lambda^3 + \left(\frac{b_2}{b_0}\right)'\lambda^2 + \left(\frac{b_3}{b_0}\right)'\lambda + \left(\frac{b_4}{b_0}\right)'}{4\lambda^3 + \frac{3b_1}{b_0}\lambda^2 + \frac{2b_2}{b_0}\lambda + \frac{b_3}{b_0}},$$

where

$$\left(\frac{b_1}{b_0}\right)' = -\frac{4}{T^2}, \quad \left(\frac{b_2}{b_0}\right)' = -\frac{4(2S+T)}{ST^3},$$

$$\left(\frac{b_3}{b_0}\right)' = \frac{4\alpha\delta T - 8(1+\delta S)}{ST^3}, \quad \left(\frac{b_4}{b_0}\right)' = -\frac{8(1-\alpha)\delta}{ST^3}.$$

Since $\omega_* = b_3^*/b_1^*$, we get

$$\left(\frac{d\lambda}{dT}\right)_{\lambda = i\omega_*} = \frac{1}{2}\frac{\left[\left(\frac{b_1}{b_0}\right)'^*\left(\frac{b_3^*}{b_0^*}\right) - \left(\frac{b_1^*}{b_0^*}\right)\left(\frac{b_3}{b_0}\right)'^*\right] i\omega_* + \left(\frac{b_2}{b_0}\right)'^*\left(\frac{b_3^*}{b_0^*}\right) - \left(\frac{b_1^*}{b_0^*}\right)\left(\frac{b_4}{b_0}\right)'^*}{\left[\left(\frac{b_1^*}{b_0^*}\right)\left(\frac{b_2^*}{b_0^*}\right) - 2\left(\frac{b_3^*}{b_0^*}\right)\right] i\omega_* - \left(\frac{b_1^*}{b_0^*}\right)\left(\frac{b_3^*}{b_0^*}\right)} \tag{16}$$

Multiplying both the numerator and the denominator of (16) by the conjugate of the denominator, and using $b_0^* b_3^{*2} = b_1^* b_2^* b_3^* - b_1^{*2} b_4^*$, we obtain

$$\operatorname{Re}\left(\frac{d\lambda}{dT}\right)_{\lambda = i\omega_*} = \frac{1}{2}\frac{-\frac{b_3^*}{b_0^*}\left[\frac{\Delta_4^3(T)}{b_0^3}\right]'_{T=T_*}}{\frac{b_3^*}{b_0^{*4} b_1^*}\left[b_1^{*3} b_3^* + (b_1^* b_2^* - 2b_0^* b_3^*)^2\right]} = -\frac{b_0^{*3} b_1^* \left[\frac{\Delta_4^3(T)}{b_0^3}\right]'_{T=T_*}}{2\left[b_1^{*3} b_3^* + (b_1^* b_2^* - 2b_0^* b_3^*)^2\right]},$$

where

$$\left[\frac{\Delta_4^3(T)}{b_0^3}\right]'_{T=T_*} = \frac{\Delta_4^{3\prime}(T_*) b_0^* - 3\Delta_4^3(T_*) b_0'^*}{b_0^{*4}}.$$

Finally, we prove that $\lambda = i\omega_*$ is a simple root. Otherwise both $i\omega_*$ and $-i\omega_*$ are multiple roots, and since the polynomial is fourth degree, it has to be

$$b_0 (\lambda - i\omega)^2 (\lambda + i\omega)^2 = b_0(\lambda^2 + \omega^2)^2$$

without linear and cubic terms, which is impossible**.** The previous analysis can be summarized as follows.

Theorem 2 *Assume* $\alpha < (1 + \delta S)/(\delta T)$ *and* $\Delta_4^3(T) > 0$*. Then the equilibrium point* k_* *of* (2) *is locally asymptotically stable. If there exists* $T = T_*$ *such that* $\Delta_4^3(T_*) = 0$ *and* $\Delta_4^{3\prime}(T_*)b_0^* - 3\Delta_4^3(T_*)b_0^{\prime *} < 0$*, then a Hopf bifurcation occurs at* k_* *as* T *passes through* T_**.*

We specify the parameter values as $s = 0.3$, $\alpha = 0.5$ and $\delta = 0.1$ with which we numerically confirm Theorem 2.[1] In Figure 1(A), the upward sloping solid curve describes $\Delta_4^3(S, T) = 0$ that divides the parameter region of (T, S) into two subregions, one is the white region to the left of the curve in which the equilibrium point is stable (i.e., $\Delta_4^3(S, T) > 0$) and the other is the gray region to the right in which the equilibrium point is unstable (i.e., $\Delta_4^3(S, T) < 0$). Since dynamics of the equilibrium is switched to instability from stability when the delay S crosses the curve from left to right, this curve is called the *stability switching curve*. The upward dotted line is the locus of $b_3 = 0$ that is in the gray unstable region, implying that $b_3 > 0$ in the white stable region except at point $(1/\alpha\delta, 0)$ where $\Delta_4^3(S, T) = 0$ and $b_3 = 0$. In order to perform numerical simulations we apply the linear chain trick technique,[2] which allows one to replace an equation with gamma distributed delay kernels by an equivalent system of differential equations. In consequence, the delay differential equation (2) with $m = 0$ and $n = 1$ becomes a dynamic system of four ordinary differential equations

$$\begin{cases} \dot{k}(t) &=& su(t)^\alpha - \delta v(t), \\ \dot{u}(t) &=& \dfrac{1}{S}(k(t) - u(t)), \\ \dot{v}(t) &=& \dfrac{2}{T}(z(t) - v(t)), \\ \dot{z}(t) &=& \dfrac{2}{T}(k(t) - z(t)) \end{cases} \tag{17}$$

where

$$\dot{k}(t) = s\left[\int_{-\infty}^{t} \frac{1}{S}e^{-\frac{1}{S}(t-r)}k(r)dr\right]^\alpha - \delta \int_{-\infty}^{t} \left(\frac{2}{T}\right)^2 (t - r)e^{-\frac{2}{T}(t-r)}k(r)dr,$$

and new variables are defined by

$$u(t) = \int_{-\infty}^{t} \frac{1}{S}e^{-\frac{1}{S}(t-r)}k(r)dr, \quad v(t) = \int_{-\infty}^{t} \left(\frac{2}{T}\right)^2 (t-r)e^{-\frac{2}{T}(t-r)}k(r)dr \text{ and } z(t) = \int_{-\infty}^{t} \frac{2}{T}e^{-\frac{2}{T}(t-r)}k(r)dr,$$

[1] This parameter specification is used repeatedly in the following numerical analysis.
[2] See MacDonald (1978).

Selecting two points on the stability switching curve, $a = (T_a, S_a)$ and $b = (T_b, S_b)$, each of which is denoted by the black dot in Figure 1(A), we obtain corresponding two cycles in Figure 1(B), the real curve for (T_a, S_a) and the dotted curve for (T_b, S_b).

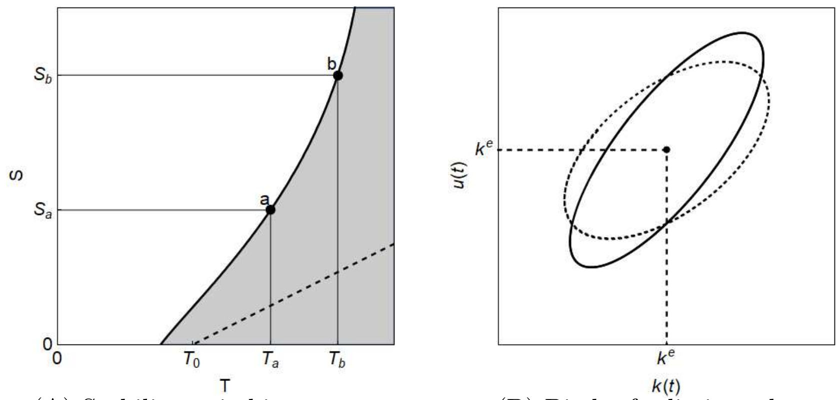

(A) Stability switching curve (B) Birth of a limit cycle

Figure 1. Dynamics of (2) with $m = 0$ and $n = 1$

3.2 Case $m = 0$ and $n \to \infty$

When n becomes infinity large, the characteristic equation (10) reduces to

$$\lambda^2 + \frac{1}{S}\lambda - \frac{\alpha\delta}{S} + \left(\frac{\delta}{S} + \delta\lambda\right) e^{-\lambda T} = 0. \tag{18}$$

In absence of delay, i.e. $T = 0$, Eq. (18) becomes

$$\lambda^2 + \left(\frac{1}{S} + \delta\right)\lambda + \frac{(1-\alpha)\delta}{S} = 0.$$

Hence the equilibrium point k_* of (2) is locally asymptotically stable since its coefficients are both positive. We take $T > 0$ and examine whether the stability switch takes place. If $\lambda = i\omega$ is a root of (18) with $\omega > 0$, then substituting it into (18), and separating the real and imaginary parts, we arrive at the following two equations

$$\begin{cases} \omega^2 + \dfrac{\alpha\delta}{S} &= \dfrac{\delta}{S}\cos\omega T + \delta\omega\sin\omega T, \\ \dfrac{1}{S}\omega &= \dfrac{\delta}{S}\sin\omega T - \delta\omega\cos\omega T. \end{cases} \tag{19}$$

Squaring both sides, adding the two equations and regrouping by powers of ω, we get

$$\omega^4 - \left(\frac{\delta^2 S^2 - 2\alpha\delta S - 1}{S^2}\right)\omega^2 - \frac{(1-\alpha^2)\delta^2}{S^2} = 0, \tag{20}$$

It is easy to see that Eq. (20) has a unique positive root ω_0, where

$$\omega_0 = \sqrt{\frac{\delta^2 S^2 - 2\alpha\delta S - 1 + \sqrt{\left(\delta^2 S^2 - 2\alpha\delta S - 1\right)^2 + 4(1-\alpha^2)\delta^2 S^2}}{2S^2}}. \tag{21}$$

Thus, Eq. (18) has a unique pair of purely imaginary roots $\pm i\omega_0$. Solving Eqs. (19) for $\sin\omega T$ and $\cos\omega T$ yields

$$\cos\omega T = \frac{\alpha}{1+S^2\omega^2} \tag{22}$$

and

$$\sin\omega T = \frac{S^2\omega^3 + (1+\alpha\delta S)\omega}{\delta(1+S^2\omega^2)}.$$

The critical values $T(j)$ of T for which the characteristic equation (18) has purely imaginary roots can be determined from (22), and they are given by

$$T(j) = \frac{1}{\omega_0}\left[\cos^{-1}\left(\frac{\alpha}{1+S^2\omega_0^2}\right) + 2j\pi\right], \quad j = 0, 1, 2, ... \tag{23}$$

Proposition 1 *Eq.* (18) *has a pair of simple purely imaginary roots* $\pm i\omega_0$ *at* $T = T(j)$. *Moreover,*

$$\left.\frac{d\,(Re\lambda)}{dT}\right|_{T=T(j)} > 0.$$

Proof. Let $\lambda(T) = \nu(T) + i\omega(T)$ and denote the root of Eq. (18) such that $\nu(T(j)) = 0$ and $\omega(T(j)) = \omega_0$. Plugging $\lambda(T(j))$ into (18) ,and taking the derivative with respect to T, one has

$$\left[2S\lambda + 1 + \delta Se^{-\lambda T} - (\delta + \delta S\lambda)\,Te^{-\lambda T}\right]\frac{d\lambda}{dT} = (\delta + \delta S\lambda)\,\lambda e^{-\lambda T}. \tag{24}$$

It is straightforward from (24) that $\lambda = i\omega_0$ is a simple root of (18). If we assume $\lambda = i\omega_0$ to be a repeated root, then $(\delta + \delta Si\omega_0)\,i\omega_0 e^{-i\omega_0 T} = 0$, leading to a contradiction. From (24), we obtain

$$\left(\frac{d\lambda}{dT}\right)^{-1} = \frac{(2S\lambda+1)\,e^{\lambda T} + \delta S}{(\delta+\delta S\lambda)\lambda} - \frac{T}{\lambda}.$$

Therefore,

$$\begin{aligned} sign\left\{\left.\frac{d\,(Re\lambda)}{dT}\right|_{T=T_j}\right\} &= sign\left\{Re\left.\left(\frac{d\lambda}{dT}\right)^{-1}\right|_{T=T_j}\right\} \\ &= sign\left\{-\delta^2S^2 + 2\alpha\delta S + 1 + 2S^2\omega_0^2\right\} \\ &= sign\left\{\sqrt{\left(\delta^2S^2 - 2\alpha\delta S - 1\right)^2 + 4(1-\alpha^2)\delta^2S^2}\right\} > 0. \end{aligned}$$

■

In conclusion, we have the following result.

Theorem 3 *Let* $T(0)$ *be defined as in* (23). *The equilibrium point* k_* *of* (2) *is locally asymptotically stable when* $\tau \in [0, T(0))$ *and unstable when* $T > T(0)$. *Furthermore,* (1) *undergoes Hopf bifurcations at the equilibrium when* $T = T(0)$.

3.3 $m = 0$ and $n = 2, 3, 4, 5$

In two cases, $m = 0$ and $n = 0$ and $m = 0$ and $n = 1$, we showed the destabilizing effect of the delay and the birth of a cyclic oscillation just when stability was lost. We now draw attention to various values of n to see how changing the from of the weighting function affects dynamics. A larger n graphically means that higher weights are concentrated to a smaller neighborhood of the maximum point $t - T$ indicating less uncertainty in the length of the delay. The degree of the characteristic equation becomes larger and so does the order of the leading principal minors of the corresponding Routh-Hurwitz determinant. It then follows that the stability condition become increasingly untractable. However we can numerically check the stability conditions. Δ_{n+3}^{k} is already defined as the k-th order leading principal minor of the Routh-Hurwitz determinant Δ_{n+3}. We illustrate the stability switching curves of $\Delta_{n+3}^{n+2} = 0$ for $n = 0, 1, 2, 3, 4, 5$ in Figure 2.[3] The right most curve corresponds to the stability switching curve in the case of $n = 0$ and so does the left most boundary of the gray region in the case of $n = 5$. It is seen that the stability switching curve shifts leftward and its slope gets steeper as n increases. It is also confirmed that given n, the equilibrium point is stable to the left of the corresponding stability switching curve and unstable to the right. The gray color becomes darker as n increases. Thus the most light-gray region corresponds to the instability region with $n = 0$. The darker gray region surrounded by the right most curve and the next right most curve is added to it to construct the instability region with $n = 1$. The instability regions with $n \geq 2$ are obtained in the same way, implying that the instability region becomes larger as n increases. In addition to these, the stability switching curve (23) with $j = 0$ in the case of $n \to \infty$ is illustrated as the left most curve. We summarize the results as follows.

Proposition 2 *Given $m = 0$, when the value of n increases from 0 to 5, the stability switching curve shift leftward as n increases, implying that increasing n has a destabilizing effect and shrinks the size of the stability region.*

and

Proposition 3 *Given $m = 0$, when $n \to \infty$, the corresponding stability switching curve is located at left most, implying that the dynamic system with continuously distributed time delay is more stable than the dynamic system with fixed time delay in the sense that the stability region of the former is larger.*

[3] For $n \leq 5$, it is numerically confirmed, as we did in Section 3.1, that $\Delta_{n+3}^{n+2} > 0$ is sufficient to have $\Delta_{n+3}^{k} > 0$ for $k = 2, 3, ..., n + 1$. Notice that $\Delta_{n+3}^{n+2} > 0$ always leads to $\Delta_{n+3}^{n+3} = (1 - \alpha)\delta\Delta_{n+3}^{n+2} > 0$.

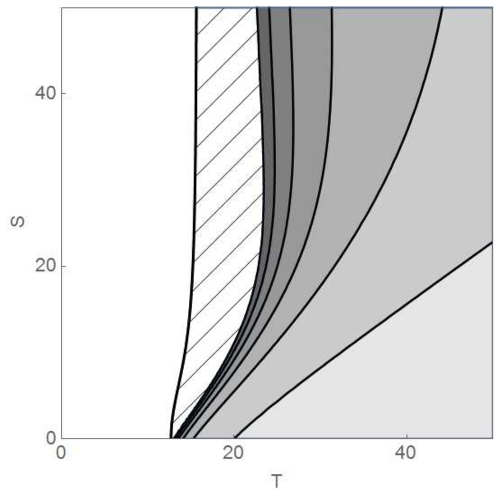

Figure 2. Stability switching curves for $m = 0,\ n = 0, 1, 2, 3, 4, 5$ and $n = \infty$

4 Heterogenous weights II: $m \geq 1$ and $n = 0$

In this section we draw attention to effects caused by increasing the value of m. To this end, we take $n = 0$ that is then substituted into the characteristic equation (5) to have the form

$$\lambda - \alpha\delta \left(1 + \frac{\lambda S}{m+1}\right)^{-(m+1)} + \delta \left(1 + \lambda T\right)^{-1} = 0.$$

Expanding the factored terms and collecting the terms in order of the powers of λ, we have a polynomial equation of degree $m + 3$,

$$b_0 \lambda^{m+3} + b_1 \lambda^{m+2} + \cdots + b_{m+2} \lambda + b_{m+3} = 0 \tag{25}$$

where the coefficients are defined by

$$\begin{aligned}
b_0 &= a_0 T, \\
b_1 &= a_1 T + a_0, \\
b_k &= a_k T + a_{k-1} + \delta a_{k-2} \text{ for } 2 \leq k \leq m+1, \\
b_{k+2} &= 1 + \delta S - \alpha\delta T, \\
b_{k+3} &= (1 - \alpha)\delta,
\end{aligned}$$

with

$$a_k = \left(\frac{S}{m+1}\right)^{m+1-k} \begin{pmatrix} m+1 \\ k \end{pmatrix}. \tag{26}$$

Comparing equation (25) having the coefficients in (26) with equation (10) having the coefficients in (11) reveals the similarities among them. In consequence, analytical methodologies become similar.

To avoid unnecessary repetition, we simplify the analysis as much as possible if the similarities are observed.

4.1 Case $m = 1$ and $n = 0$

In this section, we examine the case of $m = 1$ and $n = 0$ under which the characteristic equation (25) becomes a quartic equation

$$b_0\lambda^4 + b_1\lambda^3 + b_2\lambda^2 + b_3\lambda + b_4 = 0 \tag{27}$$

where

$$\begin{aligned} b_0 &= \frac{1}{4}S^2T > 0, \\ b_1 &= ST + \frac{1}{4}S^2 > 0, \\ b_2 &= T + S + \frac{1}{4}\delta S^2 > 0, \\ b_3 &= 1 + \delta S - \alpha\delta T, \\ b_4 &= (1-\alpha)\delta > 0. \end{aligned}$$

The locus of $b_3 = 0$ is positively sloping in the (T, S) plane whereas the slope of the $\Delta_4^3 = 0$ curve is ambiguous. Both curves pass through point $(T_0, 0)$. It is clearly seen that $b_3 \leq 0$ implies $\Delta_4^3 < 0$. The contraposition of the last statement is that $\Delta_4^3 \geq 0$ implies $b_3 > 0$. Furthermore, $\Delta_4^3 > 0$ implies $\Delta_4^2 > 0$. Hence, by the Routh-Hurwitz criterion, the stability condition is $\Delta_4^3 > 0$. Solving $\Delta_4^3 = 0$ for b_3 and then substituting the resultant solution into (27) we have the factored from of the quartic equation,

$$\left(b_1\lambda^2 + b_3\right)\left(b_0b_1\lambda^2 + b_1^2\lambda + b_1b_2 - b_0b_3\right) = 0. \tag{28}$$

The equation has two purely imaginary solutions and two other solutions

$$\lambda_{1,2} = \pm i\beta \text{ with } \beta = \sqrt{\frac{b_3}{b_1}}$$

and

$$\lambda_{3,4} = \frac{-b_1^2 \pm \sqrt{b_1^4 - 4b_0b_1\left(b_1b_2 - b_0b_3\right)}}{2b_0b_1}.$$

where $\lambda_3 < 0$ and $\lambda_4 < 0$ if the discriminant of the second solution is positive and $\mathrm{Re}\left[\lambda_{3,4}\right] < 0$ if it is negative.

Since we can check the transversality condition in the same way as in the case of $m = 0$ and $n = 1$, we omit the detail and jump to the following result:

Theorem 4 *Given a value of T, the equilibrium point k_* of (2) is locally asymptotically stable for $S < S_*$ and unstable for $S > S_*$ whereas it bifurcates to a limit cycle through a Hopf bifurcation for $S = S_*$ where S_* solves*

$$b_1b_2b_3 - b_0b_3^2 - b_1^2b_4 = 0.$$

We now numerically examine dynamic behavior of the unstable equilibrium. The dynamic system under the investigation consists of the four ordinary differential equations

$$\begin{cases} \dot{k}(t) = su(t)^a - \delta v(t), \\ \dot{v}(t) = \dfrac{1}{T}\left(k(t) - v(t)\right), \\ \dot{u}(t) = \dfrac{2}{S}\left(z(t) - u(t)\right), \\ \dot{z}(t) = \dfrac{2}{S}\left(k(t) - z(t)\right), \end{cases}$$

where the capital accumulation is described by

$$\dot{k}(t) = s\left[\int_{-\infty}^{t}\left(\frac{2}{S}\right)^2 (t-r)e^{-\frac{2}{S}(t-r)}k(r)dr\right]^{\alpha} - \delta\int_{-\infty}^{t}\frac{1}{T}e^{-\frac{1}{T}(t-r)}k(r)dr,$$

and new variables are defined by

$$v(t) = \int_{-\infty}^{t}\frac{1}{T}e^{-\frac{1}{T}(t-r)}k(r)dr,\ u(t) = \int_{-\infty}^{t}\left(\frac{2}{S}\right)^2(t-r)e^{-\frac{2}{S}(t-r)}k(r)dr \text{ and } z(t) = \int_{-\infty}^{t}\frac{2}{S}e^{-\frac{2}{S}(t-r)}k(r)dr.$$

Selecting two points, $A = (T_A, S_A)$ and $B = (T_B, S_B)$, on the stability switching curve, the points are denoted by the black dots in Figure 3(A). The resultant cycles are illustrated in Figure 3(B). The smaller cycle is obtained at point A and the larger cycle at point B.

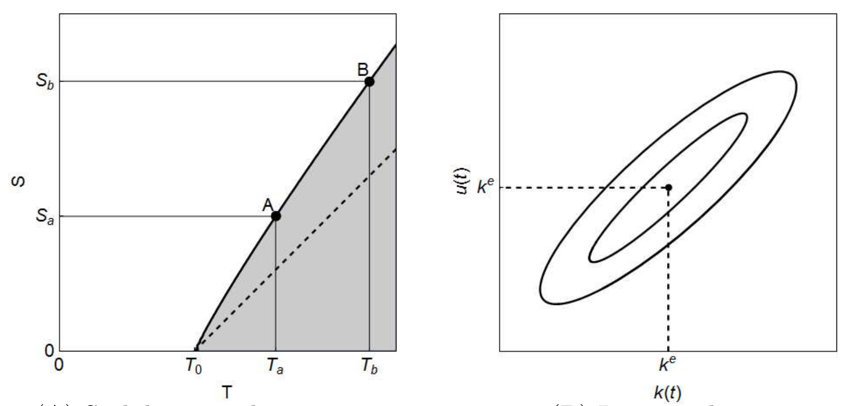

(A) Stability switching curve (B) Limit cycles

Figure 3. $m = 1$ and $n = 0$

4.2 Case $m \to \infty$ and $n = 0$

When the value of m is infinitely large, the characteristic equation (5) turns to be

$$\lambda - \alpha\delta e^{-\lambda S} + \delta(1 + \lambda T)^{-1} = 0.$$

In case of no fixed delay (i.e., $S = 0$), it is reduced to

$$\lambda - \alpha\delta + \delta(1 + \lambda T)^{-1} = 0$$

or

$$T\lambda^2 + (1 - \alpha\delta T)\lambda + (1 - \alpha)\delta = 0.$$

If $T < 1/\alpha\delta = T_0$, then all coefficients are positive and thus the equilibrium point k_* is locally asymptotically stable.

Now let $S > 0$. The characteristic equation is

$$\lambda^2 + \frac{1}{T}\lambda + \frac{\delta}{T} - \alpha\delta\left(\frac{1}{T} + \lambda\right)e^{-\lambda S} = 0. \tag{29}$$

Suppose that $\lambda = i\omega,\ \omega > 0$, is a root of (29) for some S. Substituting it into (29) and separating the real and imaginary parts yield

$$\begin{aligned} \alpha\delta\cos\omega S + \alpha\delta\omega T\sin\omega S &= -\omega^2 T + \delta, \\ \alpha\delta\sin\omega S - \alpha\delta\omega T\cos\omega S &= -\omega. \end{aligned} \tag{30}$$

Adding the squared terms presents the quartic equation in ω,

$$T^2\omega^4 + \left[1 - 2\delta T - (\alpha\delta T)^2\right]\omega^2 + (1 - \alpha^2)\delta^2 = 0. \tag{31}$$

Its roots are

$$\omega_\pm^2 = \frac{(\alpha\delta T)^2 + 2\delta T - 1 \pm \sqrt{D}}{2T^2}$$

where the discriminant D has the following form

$$D = \left[(\alpha\delta T)^2 + 2\delta T - 1\right]^2 - 4(1 - \alpha^2)\delta^2 T^2. \tag{32}$$

Solving $(\alpha\delta T)^2 + 2\delta T - 1 = 0$ for T gives the threshold value of T,

$$\bar{T} = T_0\frac{-1 + \sqrt{1 + \alpha^2}}{\alpha}\left(< T_0 = \frac{1}{\alpha\delta}\right)$$

such that $(\alpha\delta T)^2 + 2\delta T - 1 > 0$ for $T > \bar{T}$. It is confirmed that $D > 0$ if $T_1 < T < T_2$ where T_1 and T_2 solve $D = 0$ and are given by

$$T_1 = T_0\frac{\sqrt{1 + \sqrt{1 - \alpha^2}\left(\sqrt{2} - \sqrt{1 + \sqrt{1 - \alpha^2}}\right)}}{\alpha} < T_0$$

and

$$T_2 = T_0\frac{\sqrt{1 - \sqrt{1 - \alpha^2}\left(\sqrt{2} - \sqrt{1 - \sqrt{1 - \alpha^2}}\right)}}{\alpha} < T_0.$$

It is also confirmed that $T_1 < \bar{T} < T_2$. Hence (31) has two imaginary solutions, $\lambda_\pm = i\omega_\pm$ with $\omega_+ > \omega_- > 0$.

We determine the sign of the derivative of $\mathrm{Re}\,[\lambda(S)]$ at the point where $\lambda(S)$ is purely imaginary. Differentiating (29) with respect to S presents

$$\left\{2\lambda + \frac{1}{T} - \alpha\delta\left[1 - S\left(\frac{1}{T} + \lambda\right)\right] e^{-\lambda S}\right\} \frac{d\lambda}{dS} = -\alpha\delta\lambda\left(\lambda + \frac{1}{T}\right) e^{-\lambda S}.$$

For convenience, we study $(d\lambda/dS)^{-1}$ instead of $d\lambda/dS$

$$\left(\frac{d\lambda}{dS}\right)^{-1} = \frac{\left(2\lambda + \dfrac{1}{T}\right) e^{\lambda S} - \alpha\delta}{-\alpha\delta\lambda\left(\lambda + \dfrac{1}{T}\right)} - \frac{S}{\lambda}.$$

Therefore

$$\begin{aligned} sign\left[\left.\frac{d(\mathrm{Re}\,\lambda)}{dS}\right|_{\lambda=i\omega}\right] &= sign\left[\mathrm{Re}\left(\left.\left(\frac{d\lambda}{dS}\right)^{-1}\right|_{\lambda=i\omega}\right)\right] \\ &= sign\left[2\left(\omega^2 - \frac{(\alpha\delta T)^2 + 2\delta T - 1}{2T^2}\right)\right] \\ &= sign\left[\pm\sqrt{D}\right]. \end{aligned}$$

Hence the sign is positive for ω_+ and negative for ω_-

$$sign\left[\left.\frac{d(\mathrm{Re}\,\lambda)}{dS}\right|_{\lambda=i\omega_+}\right] = sign\left[\sqrt{D}\right] \tag{33}$$

and

$$sign\left[\left.\frac{d(\mathrm{Re}\,\lambda)}{dS}\right|_{\lambda=i\omega_-}\right] = sign\left[-\sqrt{D}\right]. \tag{34}$$

Solving (30) gives two solutions corresponding to $\omega_\pm^2$. In particular, for ω_+ and $\theta_+ = S_+\omega_+$,

$$\cos\theta_+ = \frac{1}{\alpha\left(1 + T^2\omega_+^2\right)} > 0 \text{ and } \sin\theta_+ = -\frac{\omega_+}{\alpha\delta}\frac{1 - \delta T + T^2\omega_+^2}{1 + T^2\omega_+^2} < 0 \tag{35}$$

where the negative sign is due to

$$1 - \delta T + T^2\omega_+^2 = \frac{1 + (\alpha\delta T)^2 + \sqrt{D}}{2} > 0.$$

Hence solving the first equation of (35) yields the locus of (T, S) for which there are imaginary roots,

$$S_+(i) = \frac{1}{\omega_+}\left\{\cos^{-1}\left[-\frac{1}{\alpha\left(1 + T^2\omega_+^2\right)}\right] + (2i+1)\pi\right\} \tag{36}$$

where i denotes integer number. For ω_-^2 and $\theta_- = S_-\omega_-$,

$$\cos\theta_- = \frac{1}{\alpha\left(1+T^2\omega_-^2\right)} > 0 \text{ and } \sin\theta_- = -\frac{\omega_-}{\alpha\delta}\frac{1-\delta T+T^2\omega_-^2}{1+T^2\omega_-^2} \tag{37}$$

where

$$1-\delta T+T^2\omega_-^2 = \frac{1+(\alpha\delta T)^2-\sqrt{D}}{2}$$

and

$$D-\left[1+(\alpha\delta T)^2\right] = 4\delta T(\alpha\delta T+1)(\alpha\delta T-1).$$

The sign of $\sin\theta_-$ depends on the values of T. If $\alpha\delta T-1<0$ or $T<T_0$, then $1-\delta T+T^2\omega_-^2>0$ that in turn implies $\sin\theta_-<0$. On the other hand, if $\alpha\delta T-1>0$ or $T>T_0$, then $1-\delta T+T^2\omega_-^2<0$ that in turn implies $\sin\theta_->0$. Hence solving the first equation of (37) yields two solutions depending on whether T is less or greater than T_0. Indeed for $T<T_0$, $\cos\theta_->0$ and $\sin\theta_-<0$ implying

$$S_-^A(j) = \frac{1}{\omega_-}\left\{\cos^{-1}\left[-\frac{1}{\alpha\left(1+T^2\omega_-^2\right)}\right]+(2j+1)\pi\right\}$$

and for $T>T_0$, $\cos\theta_->0$ and $\sin\theta_->0$ implying

$$S_-^B(j) = \frac{1}{\omega_-}\left\{\cos^{-1}\left[\frac{1}{\alpha\left(1+T^2\omega_-^2\right)}\right]+2j\pi\right\}.$$

Several stability switching curves are illustrated in the first quadrant of region (S,T) in Figure 4. The red curves are described by $S_+(0)$, $S_+(1)$ and $S_+(2)$, the blue curves are defined for $T<T_0$ and described by $S_-^A(0)$, $S_-^A(1)$ and $S_-^A(2)$. Finally, the green curves are defined for $T>T_0$ and described by $S_-^B(0)$ and $S_-^B(1)$. It is also confirmed that

$$S_+(i) = S_-^A(i) \text{ and } T=T_s \text{ and } S_-^A(i) = S_-^B(i+1) \text{ at } T=T_0.$$

Hence each curve is smoothly connected at these points to construct one continuous curve.

The characteristic equation has a pair of purely imaginary roots on the curves and stability or instability change takes place there. We see the effects caused by a change in S in Figure 4 in which the equilibrium point is stable in the yellow region and unstable in the gray region. First we take $T=18$ and denote it by T_{18}. Then we obtain the multiple stability switches by increasing the value of S along the vertical line standing at $T=T_{18}$.

(i) The equilibrium point is stable for $S=0$ and loses stability at point a because the real part of one eigenvalue becomes positive for a larger value of S due to (33).

(ii) The real part of the eigenvalue becomes zero at point b and instability is switched to stability by further increases of S due to (34).

(iii) Stability is lost again at point c and never regained by a larger value of S.

Secondly we increase the value of T to 25 and denote it by T_{25}. Using the same procedure, we increase the value of S along the vertical line at $T=T_{25}$ and see how different values of S affect accumulation of the capital stock.

(i) The equilibrium point is unstable for $S = 0$ and gains stability at point A at which the positive real part of one eigenvalue, a source of instability, is zero and then the real parts of all eigenvalues are negative for a larger value of S.

(ii) Stability is lost at point B and no regain of stability is obtained for any larger values of S because the vertical line is located in the gray region.

We summarize the main results.

Proposition 4 *For $n = 0$ and $m \to \infty$, the stability switching curve is an envelop of $S_+(i)$, $S_-^B(i)$ and $S_-^B(i)$ for $i \in \mathbb{N}$ and stability loss and gain may repeat alternately if the value of τ_2 increases while the value of τ_1 is fixed at some positive value.*

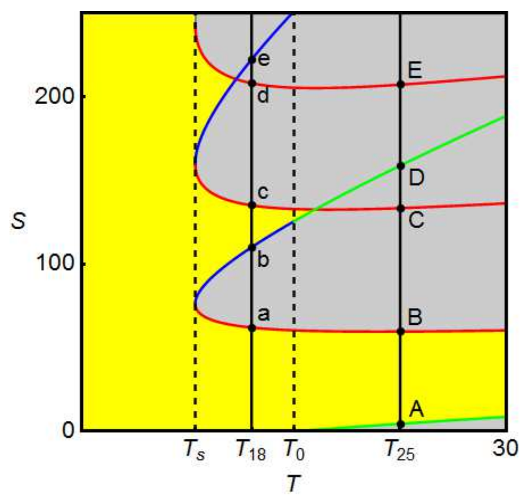

Figure 4. Stability switching curves

4.3 $m = 0, 1, 2, 3, 4, 5$ and $n = 0$

As in Section 2.3, we examine the effects caused by increasing the value of m on dynamics, fixing the value of n at zero. Increasing the value of m makes the shape of the weighting function more taller and more thinner. We illustrate six stability switching curves of Δ_{m+3}^{m+2} for $m = 0, 1, 2, 3, 4, 5$ in Figure 5 in which the steady state is stable in the gray regions on the right to the curve. It can be analytically shown that a larger m shifts the stability switching curves leftward, implying a decrease of the stability region. However the degree of the effect is so small that the curve shifts are invisible in Figure 5(A). The inside area of the small rectangle in the upper-right corner is enlarged in Figure 5(B) in which we can see the shifts of the stability switching curves. The right most curve is the stability switching curve with $m = 0$ and the left most boundary of the gray region is the stability switching curve with $m = 5$. It is seen that as the value of m increases, the stability switching curve shifts leftward. The stability switching curve in the case of $m \to \infty$ is illustrated as the left boundary of the hatched-line region. It corresponds to the lowest green curve passing point A in Figure 4, which is described by $S_-^B(0)$. We summarize the results obtained in this section, which is very similar to Proposition xx.

Proposition 5 *Given $n = 0$, when the value of n increases from 0 to 5, the stability switching curve shifts rightward as m increases, implying that increasing m has a destabilizing effect and shrinks the size of the stability region.*

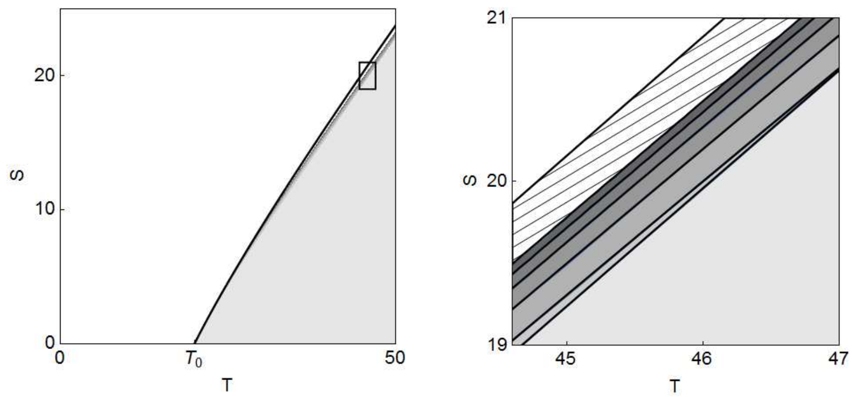

(A) Stability switching curves (B) Enlargement

Figure 5. Stability regions and shifts of the stability switching curves

5 Concluding Remarks

In this study we have focused on the effects of continuous delays on capital accumulation. Assuming that the neoclassical growth model has two different delays concerning capital, a time-to-build delay and a time-to-depreciat delay and both delays have different weighting kernels. We first show that the model with weaker kernel is more stable than the one with stronger kernel in the sense that the stability region of the former is larger. Second, in the limiting case in which the continuous delay converges to the fix delay, the model with the fix delay has the smallest stability region. Third, we analytically show the existence of a threshold value of the delay, the model is stable for the delay less than this threshold and becomes unstable for the delay larger than the threshold. Forth, we numerically demonstrate two dynamic results; one is that a cycle emerges for this threshold value and the other is that stability loss and gain may repeat alternatively, implying that the delay has a destabilizing effect as well as a stabilizing effect. Such duality of the delay never appear in one-delay models.

References

[1] Bianca, C., M. Ferrara and L. Guerrini, The time delays' effects on the qualitative behavior of an economic growth model, *Abstract and Applied Analysis*, vol. 2013, Article ID 901014, DOI: 10.1155/2013/901014, 2013.

[2] Day, R., Irregular Growth Cycles, *American Economic Review*, vol. 72, 406-414, 1982.

[3] Kalecki, M., A macrodynamic theory of business cycles, *Econometrica*, vol. 3, 327-344, 1935.

[4] Guerrini, L., Matsumoto, A., and F. Szidarovszky, Neoclassical Growth Model with Two Fixed Delays, mimeo, 2017

[5] MacDonald, N., *Time lags in biological systems*, Springer, New York, 1978.

[6] Matsumoto, A., and F. Szidarovszky, Asymptotic behavior of a delay differential neoclassical model, *Sustainability*, vol. 5, 440-455, 2013.

[7] Matsumoto, A., and F. Szidarovszky, Delay differential neoclassical growth model, *Journal of Econmic Behavior and Organization*, vol. 78, 272-289, 2011

[8] Zak, P. J., Kaleckian lags in general equilibrium, *Review of Political Economy*, vol.11, 321–330, 1999.